

## Article

# Steric, Activation Method and Solvent Effects on the Structure of Paddlewheel Diruthenium Complexes

Patricia Delgado-Martínez <sup>1</sup>, Luis Moreno-Martínez <sup>2</sup> , Rodrigo González-Prieto <sup>2,\*</sup> , Santiago Herrero <sup>2</sup> , José L. Priego <sup>2</sup> and Reyes Jiménez-Aparicio <sup>2,\*</sup> 

<sup>1</sup> Centro de Asistencia a la Investigación Difracción de Rayos X, Facultad de Ciencias Químicas, Universidad Complutense de Madrid, E-28040 Madrid, Spain; patriciadelgado@ucm.es

<sup>2</sup> Departamento de Química Inorgánica, Facultad de Ciencias Químicas, Universidad Complutense de Madrid, Ciudad Universitaria, E-28040 Madrid, Spain; luis.morenomartinez@educa.madrid.org (L.M.-M.); sherrero@ucm.es (S.H.); bermejo@ucm.es (J.L.P.)

\* Correspondence: rodgonza@ucm.es (R.G.-P.); reyesja@ucm.es (R.J.-A.)

**Featured Application:** The most studied application of diruthenium compounds is as catalysts in different chemical processes due to the possibility of diruthenium units to coordinate chemical species through their axial, equatorial or peripheral positions. However, the most promising application of these complexes is as a carrier of drugs in anticancer therapy and in the research of the structure of biomolecules.

**Abstract:** Conventional heating and solvothermal synthetic methods (with or without microwave activation) have been used to study the reaction of *o*-, *m*- and *p*-methoxybenzoic acid with [Ru<sub>2</sub>Cl(μ-O<sub>2</sub>CMe)<sub>4</sub>]. The tetrasubstituted series [Ru<sub>2</sub>Cl(μ-O<sub>2</sub>CC<sub>6</sub>H<sub>4</sub>-R)<sub>4</sub>], with R = *o*-OMe, *m*-OMe and *p*-OMe, has been prepared by the three procedures. Depending on the synthetic method and the experimental conditions, three compounds have been isolated (**1a**, **1b**, **1c**) with the *o*-methoxybenzoate ligand. However, with the *m*- and *p*-methoxybenzoate ligands, only the complexes **2** and **3** have been obtained, respectively. Compound **1a**, with stoichiometry [Ru<sub>2</sub>Cl(μ-O<sub>2</sub>CC<sub>6</sub>H<sub>4</sub>-*o*-OMe)<sub>4</sub>]<sub>n</sub>, shows a polymeric structure with the chloride ions bridging the diruthenium units to form linear chains. Compounds **2** and **3**, with the same stoichiometry, predictably form zig-zag chains in accordance with their insolubility and their magnetic measurements. Compound **1b**, [Ru<sub>2</sub>Cl(μ-O<sub>2</sub>CC<sub>6</sub>H<sub>4</sub>-*o*-OMe)<sub>4</sub>(EtOH)], is a discrete molecular species with a chloride ion and one ethanol molecule occupying the axial positions of the dimetallic unit. Compound **1c** is a cation-anion complex, [Ru<sub>2</sub>(μ-O<sub>2</sub>CC<sub>6</sub>H<sub>4</sub>-*o*-OMe)<sub>4</sub>(MeOH)<sub>2</sub>][Ru<sub>2</sub>Cl<sub>2</sub>(μ-O<sub>2</sub>CC<sub>6</sub>H<sub>4</sub>-*o*-OMe)<sub>4</sub>]. The cationic complex has two solvent molecules at the axial positions whereas the anionic complex has two chloride ligands at these positions. Complexes have been characterized by elemental analyses, mass spectrometry and IR and UV-vis-NIR spectroscopies. A magnetic study of complexes **1a**, **1b**, **2** and **3** have also been carried out. The crystal structure of compounds **1b** and **1c** have been solved by single X-ray crystal methods.

**Keywords:** diruthenium; solvothermal synthesis; microwave synthesis; carboxylate complexes; metal-metal



**Citation:** Delgado-Martínez, P.; Moreno-Martínez, L.; González-Prieto, R.; Herrero, S.; Priego, J.L.; Jiménez-Aparicio, R. Steric, Activation Method and Solvent Effects on the Structure of Paddlewheel Diruthenium Complexes. *Appl. Sci.* **2022**, *12*, 1000. <https://doi.org/10.3390/app12031000>

Academic Editor: Emiliano Principi

Received: 16 December 2021

Accepted: 17 January 2022

Published: 19 January 2022

**Publisher's Note:** MDPI stays neutral with regard to jurisdictional claims in published maps and institutional affiliations.



**Copyright:** © 2022 by the authors. Licensee MDPI, Basel, Switzerland. This article is an open access article distributed under the terms and conditions of the Creative Commons Attribution (CC BY) license (<https://creativecommons.org/licenses/by/4.0/>).

## 1. Introduction

The syntheses and properties of numerous formally mixed-valent diruthenium(II,III) complexes have been reported to date [1–3]. The synthesis and reactivity of tetracarboxylatochloridodiruthenium complexes, [Ru<sub>2</sub>Cl(μ-O<sub>2</sub>CR)<sub>4</sub>] (R = alkyl or aryl), with paddlewheel structure have been intensively studied due to their singular electronic and magnetic properties [4] and their potential applications in several fields as catalysers [5,6], anticancer drugs [7,8], drugs carriers [9] or structural probes of biomolecules [10–12]. These complexes are usually obtained by the metathesis reaction of [Ru<sub>2</sub>Cl(μ-O<sub>2</sub>CMe)<sub>4</sub>]<sub>n</sub> with an excess of the corresponding carboxylic acid in a refluxing mixture of methanol/water (1:1). In many

cases it is necessary to carry out more than one cycle of metathesis to obtain pure tetrasubstituted compounds. Reactions with *N,O*-donor ligands as amides or hydroxypyridines need more drastic reaction conditions to carry out the complete replacement of the acetate ligands in  $[\text{Ru}_2\text{Cl}(\mu\text{-O}_2\text{CMe})_4]_n$  [13–19].

Our research group has described microwave activation as a very effective synthetic method for total acetate ligands substitution in this type of compound [20–22]. In addition, the solvothermal activation produces similar substitution reactions. With microwave activation, reaction times and yields are usually better than those found in conventional heating methods. However, the most important advantage of the solvothermal synthesis is the preparation of single crystals of insoluble compounds, as is the case for tetraamidato complexes [23,24]. These alternative synthetic procedures have also been used to exchange carboxylate ligands, although in just a few examples [23,25,26]. More recently, we have shown that the reaction of  $[\text{Ru}_2\text{Cl}(\mu\text{-O}_2\text{CMe})_4]_n$  with formamides or amides activated by ultrasounds selectively gives the monosubstituted complexes [27].

In this paper, we describe the preparation of new complexes with  $[\text{Ru}_2(\mu\text{-O}_2\text{CC}_6\text{H}_4\text{-R})_4]^+$  cores:  $[\text{Ru}_2\text{Cl}(\mu\text{-O}_2\text{CC}_6\text{H}_4\text{-}o\text{-OMe})_4]_n$  (**1a**),  $[\text{Ru}_2\text{Cl}(\mu\text{-O}_2\text{CC}_6\text{H}_4\text{-}o\text{-OMe})_4(\text{EtOH})]$  (**1b**),  $[\text{Ru}_2(\mu\text{-O}_2\text{CC}_6\text{H}_4\text{-}o\text{-OMe})_4(\text{MeOH})_2][\text{Ru}_2\text{Cl}_2(\mu\text{-O}_2\text{CC}_6\text{H}_4\text{-}o\text{-OMe})_4]$  (**1c**),  $[\text{Ru}_2\text{Cl}(\mu\text{-O}_2\text{CC}_6\text{H}_4\text{-}m\text{-OMe})_4]_n$  (**2**) and  $[\text{Ru}_2\text{Cl}(\mu\text{-O}_2\text{CC}_6\text{H}_4\text{-}p\text{-OMe})_4]_n$  (**3**) using conventional heating and solvothermal methods (with or without microwave activation) in order to compare the advantages and disadvantages of these methods in the preparation of tetracarboxylatodiruthenium complexes. The synthesis and crystal structure of complex **3** has been previously described by Das and Chakravarty [28]. Two different crystalline forms of complex **1** (**1a** and **1c**) have been characterized by single crystal X-ray structural analysis. The rest of the complexes have been isolated as microcrystalline solids. The influence on these reactions of the position of the -OMe group in the phenyl ring has also been studied.

## 2. Materials and Methods

### 2.1. Materials

All reactants and solvents were acquired from commercial sources and used as received without further purification. The starting reagent  $[\text{Ru}_2\text{Cl}(\mu\text{-O}_2\text{CMe})_4]_n$  was synthesized following the general procedure described in the literature [29].

Microwave reactions were carried out in an ETHOS ONE microwave oven using TFM Teflon closed vessels equipped with a temperature sensor and pressure control. Solvothermal syntheses were carried out in a Memmert Universal Oven UFE 400 using Teflon-lined stainless steel autoclaves.

### 2.2. Physical Measurements

Elemental analyses were carried out at the Microanalytical Services of the Complutense University of Madrid. FT-IR measurements were carried out in the 4000–650  $\text{cm}^{-1}$  spectral range with a Perkin-Elmer Spectrum 100 equipped with a universal ATR accessory. The electronic spectra of the complexes in the solid state were acquired on a Cary 5G spectrophotometer equipped with a Praying Mantis accessory for diffuse reflectance measurements. The reflectance data were converted by the instrument software to the  $F(R_\infty)$  values according to the Kubelka–Munk theory. Mass spectra were recorded by the Research Interdepartmental Service (SIdI) of Universidad Autónoma de Madrid using a VG AutoSpec mass spectrometer and *m*-nitrobenzyl alcohol (*m*-NBA) as matrix. Nominal molecular masses and the isotopic distribution of all peaks were calculated using the MASAS computer program [30], using a polynomial expansion based on natural abundances of the isotopes. The variable-temperature magnetic susceptibility data were measured on a Quantum Design MPMSXL SQUID (Superconducting Quantum Interference Device) magnetometer at 0.5 T for compounds **1a**, **2** and **3** and 1 T for **1b** over a temperature range of 2–299 K. All data were corrected for the diamagnetic contribution of the samples and for the signal of the sample holder. The molar diamagnetic corrections for the complexes were calculated on the basis of Pascal's constants.

### 2.3. Crystallography

Single crystal X-ray diffraction data collection was carried out at room temperature on a Bruker Smart CCD diffractometer using graphite-monochromated Mo-K $\alpha$  ( $\lambda = 0.71073 \text{ \AA}$ ) operating at 50 kV and 35 mA for **1b** and 50 kV and 30 mA for **1c**. In both cases, data were collected over a hemisphere of the reciprocal spaceCell; parameters were determined and refined by a least-squares fit of all reflections. The first 100 frames were collected at the end of the data collection to monitor crystal decay, and no appreciable decay was observed. A semi-empirical absorption correction (SADABS23) was applied in both cases. A summary of the fundamental crystal and refinement data is given in Table 1. CCDC 2,118,574 (for **1c**) and 2,118,575 (for **1b**) contain the crystallographic data for the compounds described in this article. These data can be obtained free of charge from the Cambridge Crystallographic Data Centre via [www.ccdc.cam.ac.uk/data\\_request/cif](http://www.ccdc.cam.ac.uk/data_request/cif) (accessed on 16 December 2021).

**Table 1.** Crystal and refinement for **1b** and **1c**.

	<b>1b</b>	<b>1c</b>
Empirical formula	C <sub>34</sub> H <sub>33</sub> ClO <sub>13</sub> Ru <sub>2</sub>	C <sub>66</sub> H <sub>62</sub> Cl <sub>2</sub> O <sub>26</sub> Ru <sub>4</sub>
Formula weight	887.03	1746.33
Temperature/K	293(2)	293(2)
Crystal system	Triclinic	triclinic
Space group	<i>P</i> -1	<i>P</i> -1
<i>a</i> /Å	8.6893(9)	10.5091(13)
<i>b</i> /Å	14.4399(15)	10.6029(13)
<i>c</i> /Å	14.5070(16)	15.938(2)
$\alpha$ /°	84.308(2)	85.170(2)
$\beta$ /°	79.522(2)	75.587(2)
$\gamma$ /°	80.622(2)	84.125(2)
Volume/Å <sup>3</sup>	1761.4(3)	1707.8(4)
<i>Z</i>	2	1
$\rho_{\text{calc}}/\text{g cm}^{-3}$	1.672	1.698
$\mu/\text{mm}^{-1}$	0.998	1.028
Reflections collected	13207	12851
Independent reflections	6018 [ $R_{\text{int}} = 0.0387$ , $R_{\text{sigma}} = 0.0568$ ]	5837 [ $R_{\text{int}} = 0.0871$ , $R_{\text{sigma}} = 0.0883$ ]
Goodness-of-fit on F <sup>2</sup>	1.036	0.967
Final R indexes [ $I \geq 2\sigma(I)$ ]	R1 = 0.0488, wR2 = 0.1250	R1 = 0.0387, wR2 = 0.0861
Final R indexes [all data]	R1 = 0.0855, wR2 = 0.1438	R1 = 0.0673, wR2 = 0.1003

### 2.4. Synthesis

#### 2.4.1. Synthesis of [Ru<sub>2</sub>Cl( $\mu$ -O<sub>2</sub>CC<sub>6</sub>H<sub>4</sub>-*o*-OMe)<sub>4</sub>]<sub>n</sub> (**1a**)

The synthesis of this compound was carried out following two different methods:

*Method a: Microwave assisted solvothermal synthesis.* [Ru<sub>2</sub>Cl( $\mu$ -O<sub>2</sub>CCH<sub>3</sub>)<sub>4</sub>]<sub>n</sub> (0.12 g, 0.25 mmol), *o*-methoxybenzoic acid (0.23 g, 1.50 mmol), 8 mL of ethanol and a magnetic stirrer bar were placed into an 85 mL TFM Teflon vessel. The vessel, sealed with a lid equipped with temperature and pressure sensors, was placed in the microwave oven. The reaction mixture was then treated by a three-step program consisting of (i) 15 min heating ramp up to 100 °C, (ii) 16 h isotherm at 100 °C and (iii) 20 min cooling ramp up to room temperature. A brown solid is obtained after filtration and washing with 2 × 10 mL

of cold ethanol. Finally, it was dried under vacuum. Yield: 76%. Anal. Calcd.(%) for  $\{[\text{Ru}_2\text{Cl}(\mu\text{-O}_2\text{CC}_6\text{H}_4\text{-}o\text{-OMe})_4]\cdot\text{H}_2\text{O}\}_n$  (**1a**·H<sub>2</sub>O): C, 44.68; H, 3.52. Found (%): C, 44.39; H, 3.69.

*Method b: Conventional synthesis.* First, 0.12 g (0.25 mmol) of  $[\text{Ru}_2\text{Cl}(\mu\text{-O}_2\text{CCH}_3)_4]_n$  and 0.23 g (1.50 mmol) of *o*-methoxybenzoic acid were added to 24 mL of MeOH/H<sub>2</sub>O (1:1). The reaction mixture was refluxed for 4 h. The brown precipitate formed was obtained by filtration, washed twice with 10 mL of absolute ethanol and dried under vacuum. Yield: 53%. Anal. Calcd.(%) for  $\{[\text{Ru}_2\text{Cl}(\mu\text{-O}_2\text{CC}_6\text{H}_4\text{-}o\text{-OMe})_4]\cdot\text{H}_2\text{O}\}_n$  (**1a**·H<sub>2</sub>O): C, 44.68; H, 3.52. Found (%): C, 44.45; H, 3.58.

FT-IR (cm<sup>-1</sup>): 3073w, 3021w, 2942w, 2839w, 1608w, 1587w, 1490w, 1473w, 1446m, 1391s, 1315w, 1287m, 1247m, 1181w, 1167w, 1115w, 1085w, 1043m, 996w, 969w, 899w, 887w, 845w, 788m, 755s, 703w, 678m.

UV-Vis-NIR (diffuse reflectance): [ $\lambda$ , nm] 332sh, 450, 1088.

Mass spectrometry [ $m/z$  (fragment)]: 808  $[\text{Ru}_2(\mu\text{-O}_2\text{CC}_6\text{H}_4\text{-}o\text{-OMe})_4]^+$ .

$\mu_{\text{eff}}$  (R.T.) = 3.86  $\mu_B$ .

#### 2.4.2. Synthesis of $[\text{Ru}_2\text{Cl}(\mu\text{-O}_2\text{CC}_6\text{H}_4\text{-}o\text{-OMe})_4(\text{EtOH})]_n$ (**1b**)

*Method c: Solvothermal synthesis.* The same reagents and quantities used for the synthesis of **1a** were added to a 23 mL Teflon-lined autoclave and stirred to get a homogenous dispersion. The closed reactor was treated under a three-step program consisting of (i) 2 h heating ramp up to 100 °C, (ii) 24 h isotherm at 100 °C and (iii) 40 h cooling ramp down to room temperature. Brown, needle-shaped crystals were obtained after filtration, washed with cold absolute ethanol (2 × 10 mL) and dried under vacuum. Yield: 71%. Anal. Calcd.(%) for  $[\text{Ru}_2\text{Cl}(\mu\text{-O}_2\text{CC}_6\text{H}_4\text{-}o\text{-OMe})_4(\text{EtOH})]\cdot\text{H}_2\text{O}$  (**1b**): C, 45.06; H, 4.00. Found (%): C, 45.19; H, 3.80.

FT-IR (cm<sup>-1</sup>): 3117w, 2978w, 2945w, 2842w, 2184w, 1600m, 1581m, 1492m, 1469m, 1437m, 1387s, 1328w, 1295w, 1276m, 1251s, 1183m, 1166m, 1149m, 1105m, 1042m, 1019m, 937w, 876w, 852m, 788w, 752s, 705w, 670s.

$\mu_{\text{eff}}$  (R.T.) = 4.17  $\mu_B$ .

#### 2.4.3. Synthesis of $[\text{Ru}_2(\mu\text{-O}_2\text{CC}_6\text{H}_4\text{-}o\text{-OMe})_4(\text{MeOH})_2][\text{Ru}_2\text{Cl}_2(\mu\text{-O}_2\text{CC}_6\text{H}_4\text{-}o\text{-OMe})_4]$ (**1c**)

The synthesis of this complex was carried out following the solvothermal synthesis (method c) used to obtain **1b**, with the same reagents, quantities and conditions, but using methanol as solvent and 16 h of cooling. After filtering and washing with cold ethanol (2 × 10 mL), a blackish powder is obtained together a few amber crystals, which are manually collected for X-ray diffraction analysis. Due to the small quantity of these crystals, a more complete characterization has not been possible.

#### 2.4.4. Synthesis of $[\text{Ru}_2\text{Cl}(\mu\text{-O}_2\text{CC}_6\text{H}_4\text{-}m\text{-OMe})_4]_n$ (**2**)

This compound has been obtained by means of the three synthetic methods described for compounds **1a** and **1b**, using *m*-methoxybenzoic acid (0.23 g, 1.50 mmol). Similar conditions were used in each case, unless otherwise stated.

*Method a:* Yield: 77%. Anal. Calcd.(%) for  $\{[\text{Ru}_2\text{Cl}(\mu\text{-O}_2\text{CC}_6\text{H}_4\text{-}m\text{-OMe})_4]\cdot\text{H}_2\text{O}\}_n$  (**2**·H<sub>2</sub>O): C, 44.68; H, 3.52. Found (%): C, 44.52; H, 3.32.

*Method b:* Yield: 76%. Anal. Calcd.(%) for  $\{[\text{Ru}_2\text{Cl}(\mu\text{-O}_2\text{CC}_6\text{H}_4\text{-}m\text{-OMe})_4]\cdot 0.5\text{H}_2\text{O}\}_n$  (**2**·0.5H<sub>2</sub>O): C, 45.16; H, 3.43. Found (%): C, 45.13; H, 3.34.

*Method c:* MeOH as solvent and 16h of cooling ramp down to room temperature were used in this synthesis. Yield: 47%. Anal. Calcd.(%) for  $\{[\text{Ru}_2\text{Cl}(\mu\text{-O}_2\text{CC}_6\text{H}_4\text{-}m\text{-OMe})_4]\cdot 3\text{H}_2\text{O}\}_n$  (**2**·3H<sub>2</sub>O): C, 42.89; H, 3.82. Found (%): C, 41.96; H, 3.38. No better elemental analysis has been obtained for the product obtained by this procedure.

FT-IR (cm<sup>-1</sup>): 3018w, 2941w, 1736w, 1587w, 1490w, 1460m, 1446m, 1398s, 1286m, 1247m, 1114w, 1043s, 787m, 755s, 678m.

UV-Vis-NIR (diffuse reflectance): [ $\lambda$ , nm] 328sh, 490, 1169.

Mass spectrometry [ $m/z$  (fragment)]: 808  $[\text{Ru}_2(\mu\text{-O}_2\text{CC}_6\text{H}_4\text{-}m\text{-OMe})_4]^+$ .

$$\mu_{\text{eff}} (\text{R.T.}) = 4.14 \mu_{\text{B.}}$$

#### 2.4.5. Synthesis of $[\text{Ru}_2\text{Cl}(\mu\text{-O}_2\text{CC}_6\text{H}_4\text{-}p\text{-OMe})_4]_n$ (**3**)

This compound has been obtained by means of the three synthetic methods described for compounds **1a** and **1b** using *p*-methoxybenzoic acid (0.23 g, 1.50 mmol). Similar conditions were used in each case, unless otherwise stated.

*Method a:* Yield: 48%. Anal. Calcd.(%) for  $[\{\text{Ru}_2\text{Cl}(\mu\text{-O}_2\text{CC}_6\text{H}_4\text{-}p\text{-OMe})_4\}\cdot\text{H}_2\text{O}]_n$  ( $3\cdot\text{H}_2\text{O}$ ): C, 44.68; H, 3.52. Found (%): C, 44.28; H, 3.39.

*Method b:* Yield: 61%. Anal. Calcd.(%) for  $[\{\text{Ru}_2\text{Cl}(\mu\text{-O}_2\text{CC}_6\text{H}_4\text{-}p\text{-OMe})_4\}\cdot\text{H}_2\text{O}]_n$  ( $3\cdot\text{H}_2\text{O}$ ): C, 44.68; H, 3.52. Found (%): C, 44.32; H, 3.33.

*Method c:* An isotherm at 90 °C and 24 h of cooling ramp down to room temperature were used in this synthesis. Yield: 79%. Anal. Calcd.(%) for  $[\{\text{Ru}_2\text{Cl}(\mu\text{-O}_2\text{CC}_6\text{H}_4\text{-}p\text{-OMe})_4\}\cdot 2\text{H}_2\text{O}]_n$  ( $3\cdot 2\text{H}_2\text{O}$ ): C, 43.67; H, 3.67. Found (%): C, 42.98; H, 3.31. No better elemental analysis has been obtained for the product obtained by this procedure.

FT-IR ( $\text{cm}^{-1}$ ): 3078w, 2935w, 2837w, 1603s, 1584w, 1517w, 1443w, 1388s, 1314m, 1255s, 1168s, 1107w, 1019m, 847m, 784w, 771s, 699m.

UV-Vis-NIR (diffuse reflectance):  $[\lambda, \text{nm}]$  352, 474, 1162.

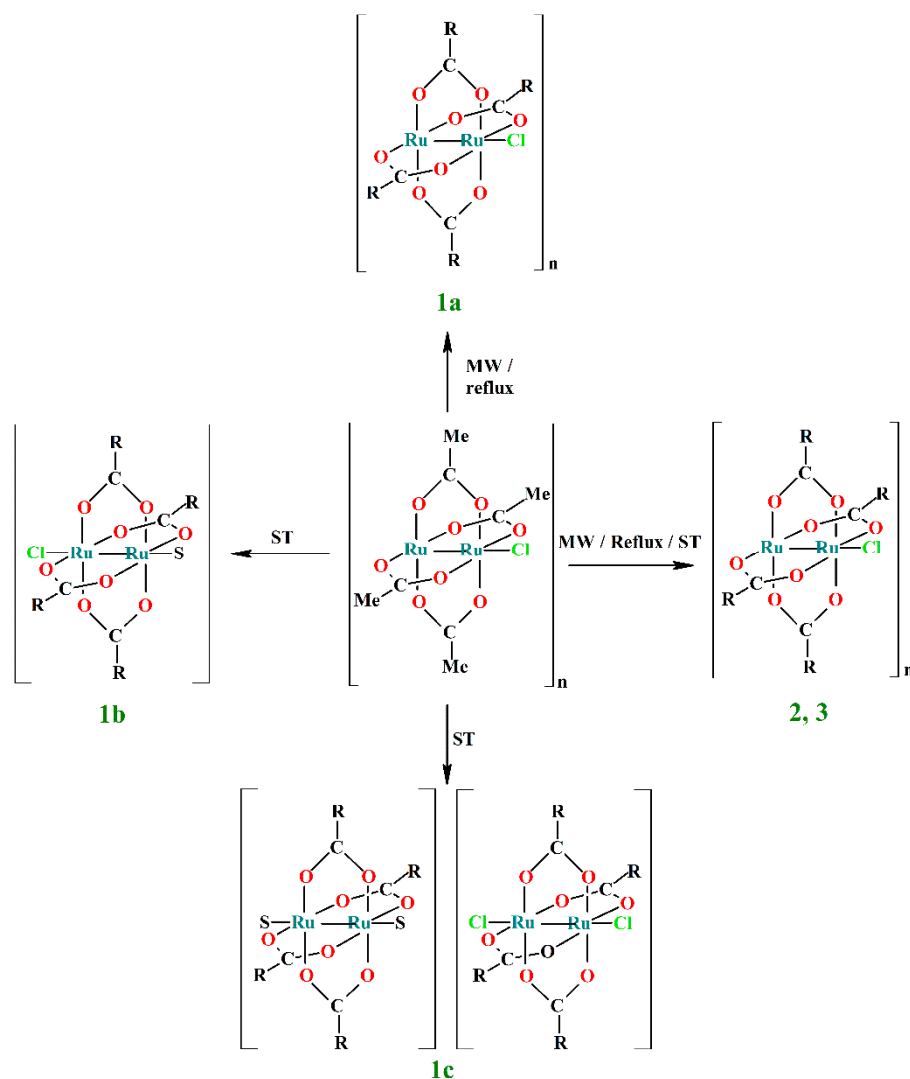
Mass spectrometry [ $m/z$  (fragment)]: 808  $[\text{Ru}_2(\mu\text{-O}_2\text{CC}_6\text{H}_4\text{-}p\text{-OMe})_4]^+$ .

$$\mu_{\text{eff}} (\text{R.T.}) = 4.07 \mu_{\text{B.}}$$

### 3. Results and Discussion

#### 3.1. Synthesis

Three synthetic methods have been used to obtain compounds  $[\text{Ru}_2\text{Cl}(\mu\text{-O}_2\text{CC}_6\text{H}_4\text{-}R)_4]_n$ , with R = *o*-OMe (**1a**, **1b**, **1c**), *m*-OMe (**2**) and *p*-OMe (**3**): (a) microwave assisted solvothermal synthesis, (b) conventional synthesis and (c) solvothermal synthesis. These methods make possible the complete replacement of the four acetate groups in the starting compound  $[\text{Ru}_2\text{Cl}(\mu\text{-O}_2\text{CCH}_3)_4]_n$  by the corresponding methoxybenzoate group. In all cases, a 50% excess of the methoxybenzoic ligand was used to favor the reaction. The preparation of compounds **1a**, **1b** and **1c** depends on the synthetic method or the experimental conditions, such as the solvent or the cooling time, whereas compounds **2** and **3** have been obtained by the three methods. The microwave assisted solvothermal method allowed the synthesis of compounds **1a**, **2** and **3** with yields of 76, 77 and 48%, respectively. Conventional metathesis reactions in MeOH/H<sub>2</sub>O (1:1) under reflux conditions also yielded compounds **1a**, **2** and **3** (yields = 53, 76 and 61%, respectively). In the three cases, due to the insolubility of the product, only one metathesis cycle was enough to get a pure phase of the compound. Solvothermal synthesis was valid to obtain compounds **2** and **3**. Although the solvothermal synthesis is a very useful method to obtain single crystals, it very often leads to a mixture of complexes. In this work, the elemental analyses of complexes **2** and **3** obtained by this method could indicate that these compounds are not very pure. For this reason, the best characterization data of **2** and **3** have been obtained with the samples prepared by conventional heating. On the other hand, using solvothermal activation with the *o*-methoxybenzoate ligand did not make possible obtaining compound **1a**; compounds **1b** and **1c** were obtained instead. In this method, slight differences in the reaction conditions have been used to obtain each compound with the best yield. In this way, compound **2** was obtained in methanol applying an isotherm of 100 °C and 16 h of cooling ramp (yield = 76%). In the synthesis of compound **3**, 90 °C, ethanol and a cooling ramp of 24 h (yield = 61%) have been used. Compound **1b** was synthesized with a good yield (71%) at 100 °C in ethanol and a cooling ramp of 40 h. However, only a few crystals of compound **1c** were obtained in a similar reaction in methanol at 100 °C and 16 h of cooling. Scheme 1 summarizes the synthetic methods used to obtain compounds **1a**, **1b**, **1c**, **2** and **3**.



**Scheme 1.** Synthetic methods employed to synthesize compounds **1a** ( $R = C_6H_4\text{-}o\text{-OMe}$ ), **1b** ( $R = C_6H_4\text{-}o\text{-OMe}$ ,  $S = EtOH$ ), **1c** ( $R = C_6H_4\text{-}o\text{-OMe}$ ,  $S = MeOH$ ), **2** ( $R = C_6H_4\text{-}m\text{-OMe}$ ) and **3** ( $R = C_6H_4\text{-}p\text{-OMe}$ ).

Moderate or high yields were obtained except for compound **1c**, and there are no appreciable differences between the synthetic methods. This seems to indicate that microwave activation does not improve the yield in relation to conventional methods, as it has been previously observed for the synthesis of other diruthenium(II,III) complexes [20,21,23–26]. Nevertheless, the microwave method allows the use of ethanol as solvent, which is less toxic and contaminant than the methanol required in the conventional synthesis. Long-time controlled cooling ramps up to room temperature of the solvothermal syntheses have allowed the formation of single crystals of compounds **1b** and **1c**. The use of the solvothermal synthesis to get single crystals of insoluble products is well known and it has been previously described for diruthenium derivatives [23–26]. The rest of products (**1a**, **2** and **3**) have been obtained as microcrystalline solids. However, single crystals of compound **3** were obtained previously from the reaction mixture by diffusion of methanolic solutions of *p*-methoxybenzoic acid and  $[Ru_2Cl(\mu-O_2CMe)_4]_n$  [28]. The insolubility of compounds **1a**, **2** and **3** in the most usual solvents, indicates a polymeric nature as it is usual in the major part of the tetracarboxylatochloridodiruthenium(II,III) compounds [1,2,4]. The polymeric nature of complex **3** was confirmed by Das and Chakravarty [28].

The position of the methoxy group in the methoxybenzoate ligand also plays an important role in the substitution process. In all cases, the electronic effect can be neglected

because the differences must be minimal. However, the steric hindrance must be much more important. Thus, when the substituent is located in *meta* or *para* positions, there are no differences in the substitution process; only one compound is obtained. However, when the -OMe group is located in *ortho*, with a greater steric hindrance, three different arrangements of the diruthenium units have been observed depending on the reaction conditions.

### 3.2. Crystal Structures

The crystal structures of complexes **1b** and **1c** have been solved by single crystal X-ray methods. Both compounds adopt a paddlewheel arrangement with the two ruthenium atoms connected by four bridging carboxylate ligands. Thus, each Ru atom shows a distorted octahedral environment having a RuO<sub>4</sub> (carboxylates) environment in the equatorial positions and the axial sites occupied by one chloride ligand or solvent molecule and by the other Ru atom of the bimetallic unit (Figures 1 and 2).

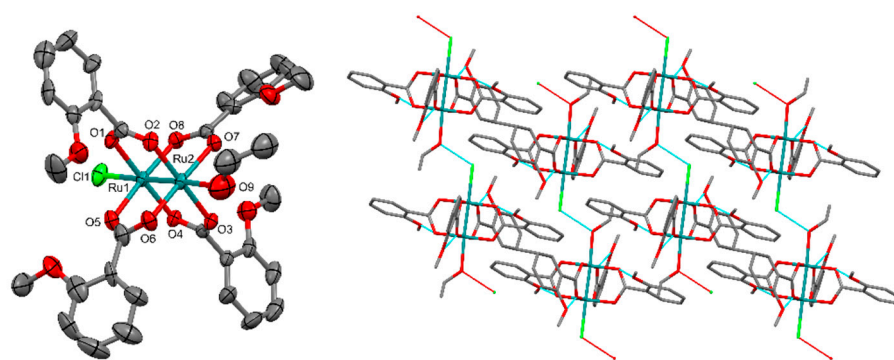


**Figure 1.** (Left) Dimetallic unit of complex **1b**. Ellipsoids are drawn at 50% probability level. (Right) Packing of compound **1b** viewed along crystallography *b* axis. Hydrogen atoms and atoms involved in disorder are omitted for clarity.

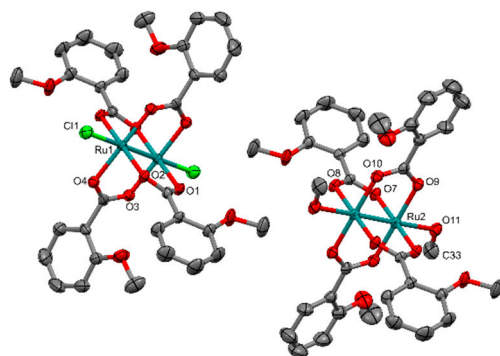


**Figure 2.** Bimetallic complexes of compound **1c**. Ellipsoids are drawn at 50% probability level. Hydrogen atoms are omitted for clarity.

Compound **1b** is formed by single bimetallic molecules that have two different axial ligands: chloride and ethanol (Figure 1 Left). This structure displays a degree of disorder concerning the positions of the carbon atoms in the rings C2–C7 and C18–C23.

This compound shows a 1D supramolecular ordering. Chains are formed along the *a*-axis through hydrogen bonds between the chloride axial ligand of a bimetallic unit and the ethanol axial ligand of the adjacent unit (Figure 1 Right).

Complex **1c** is a salt with anionic and cationic diruthenium units. The cationic complex has methanol molecules at the axial positions, whereas in the anionic complex these positions are occupied by chloride ligands (Figure 2).

In complex **1c**, both dimetallic units are bridged by solvent molecules through hydrogen bonds, giving rise to chains (Figure 3) in a similar way to the supramolecular packing observed in compound **1b**.

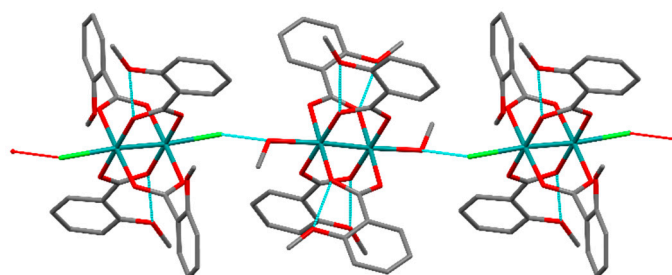


**Figure 3.** Drawing of a zigzag chain of **1c**. Hydrogen atoms are omitted for clarity.

In **1c**, the Ru–Ru distance in the anionic unit is longer than in the cationic unit [2.2950(5) and 2.2667(5) Å, respectively] due to the different donor character of the axial ligands (Table 2). These distances are very similar to those found in the complexes [Ru<sub>2</sub>Cl(μ-O<sub>2</sub>CCH<sub>2</sub>OEt)<sub>4</sub>·H<sub>2</sub>O] [2.294(2) and 2.261(1) Å] [31], and [Ru<sub>2</sub>I(μ-O<sub>2</sub>CCH<sub>2</sub>CH<sub>2</sub>OPh)<sub>4</sub>(H<sub>2</sub>O)]·0.5H<sub>2</sub>O [2.310(2) and 2.265(2) Å] [32], which form analogous anionic and cationic diruthenium complexes, in addition to zig-zag chains in the case of the former. Chloride ligands are better donors than methanol ligands and, therefore, the diruthenium atoms are richer in electronic density. Consequently, π\* and δ\* orbitals are more populated, giving a larger Ru–Ru distance. The Ru–Cl and Ru–O<sub>axial</sub> bond distances have the usual values in diruthenium complexes [1,2,4,33].

**Table 2.** Main bond distances (Å) in compounds **1b** and **1c**.

<b>1b</b>		<b>1c</b>	
Ru1–Ru2	2.2827(6)	Ru1–Ru1	2.2950(5)
Ru1–Cl1	2.508(2)	Ru2–Ru2	2.2667(5)
Ru2–O9	2.286(6)	Ru1–Cl1	2.550(1)
		Ru2–O11	2.296(3)

The Ru–Ru distance [2.2827(6)] in **1b** is in the range of the values found in compound **1c** [2.2950(5) and 2.2667(5)], which seems reasonable, taking into account the presence of chloride and ethanol axial ligands in this complex (Table 2).

In order to determine the influence of the positions of the aromatic ring in the packing of these complexes, the dihedral angle  $\theta$  has been examined. This can be defined as the angle formed by the plane of the phenyl ring and the plane occupied by COO group and the ruthenium atoms. These angles vary from 15.51° to 80.66° for compound **1c** and from 12.73° to 71.73° for **1b** (Table S1 and Figure S1, Supplementary Materials). The deviation of the methoxy group of the aromatic ring planes vary from 3.59° to 10.59° (**1c**) and 1.80° to 12.03° (**1b**) (Table S2, Supplementary Materials). These values are in a broad range and are similar in both compounds. Thus, these angles do not seem to have any significant influence on the arrangement of these complexes in the solid state.

### 3.3. Spectroscopic Properties

The infrared spectra of compounds **1–3** are very similar, and there are no appreciable differences for compounds obtained by different synthetic methods. All the spectra show the same pattern with the symmetric and antisymmetric stretching COO bands in the ranges 1398–1387 cm<sup>−1</sup> and 1446–1437 cm<sup>−1</sup>, respectively. This indicates the presence of two ruthenium atoms supported by four bridging equatorial methoxybenzoate ligands. Weak bands corresponding to the C–H stretching vibrations of the phenyl group are observed in the range 3117–3018 cm<sup>−1</sup>, and those corresponding to the methoxy substituents appear between 2978 and 2837 cm<sup>−1</sup>.

Mass spectrometry has been applied to verify the complete substitution of the acetate by the corresponding methoxybenzoate ligands in compounds **1a**, **2** and **3** [34]. Peaks

corresponding to  $[\text{Ru}_2(\mu\text{-O}_2\text{CR})_4]^+$  are observed and no peaks of partially substituted species such as  $[\text{Ru}_2(\mu\text{-O}_2\text{CMe})(\mu\text{-O}_2\text{CR})_3]^+$  or  $[\text{Ru}_2(\mu\text{-O}_2\text{CMe})_2(\mu\text{-O}_2\text{CR})_2]^+$  are found.

The diffuse reflectance electronic spectra of compounds **1a**, **2** and **3** (Table 3) show three absorption bands. The bands observed in the range 328–352 nm can be assigned to a ligand–metal charge-transfer  $\sigma(\text{axial ligand}) \rightarrow \sigma^*(\text{Ru}_2)$  transition, in accordance with the assignment made for the absorption band at 307 nm observed for the  $[\text{Ru}_2\text{I}_2(\mu\text{-O}_2\text{CPr})_4]^-$  anion [35–37]. The band found in the range 450–490 nm is mainly due to the  $\pi(\text{Ru-O, Ru}_2) \rightarrow \pi^*(\text{Ru}_2)$  transition [23,35–38] with a possible  $\sigma \rightarrow \sigma^*$  influence. Finally, the band appearing in the NIR region between 1088 and 1162 nm corresponds to a  $\delta(\text{Ru}_2) \rightarrow \delta^*(\text{Ru}_2)$  transition [23,35–41].

**Table 3.** Assignment of the absorption bands observed in the spectra of compounds **1a**, **2** and **3**.

Compound	$\sigma(\text{Axial Ligand}) \rightarrow \sigma^*(\text{Ru}_2)$	$\pi(\text{RuO, Ru}_2) \rightarrow \pi^*(\text{Ru}_2)$	$\delta(\text{Ru}_2) \rightarrow \delta^*(\text{Ru}_2)$
<b>1a</b>	332sh	450	1088
<b>2</b>	328sh	490	1169
<b>3</b>	352	474	1162

### 3.4. Magnetic Properties

The magnetic moments at room temperature of compounds **1–3** are in the range 3.86–4.17  $\mu_B$ , similar to those observed for other tetracarboxylatodiruthenium compounds [1,4,33,42]. These values are close to the theoretical value of 3.87  $\mu_B$  for three unpaired electron considering  $g = 2$ . These data are in accordance with the electronic configuration of  $\sigma^2\pi^4\delta^2(\pi^*\delta^*)^3$  per  $\text{Ru}_2^{5+}$  unit proposed by Norman et al. [43].

Compounds **1b**, **2** and **3** show similar magnetic behavior. The molar magnetic susceptibility continuously increases with decreasing temperature (300–2 K) while the magnetic moment decreases, especially at low temperature values. This behavior has been attributed to a strong zero-field splitting (D) of the diruthenium unit and a small degree of antiferromagnetic coupling (zJ) between the bimetallic units, and it is indicative of molecular or zig-zag polymeric arrangements [1,4,32,33,38,42]. The fitting of the experimental magnetic data of compounds **1b**, **2** and **3** has been carried out using the model of Cukiernik et al. [44], which takes into consideration the equations developed by O'Connor [45] and corrected later by Telser and coworkers [46]. This model takes into account the existence of D and zJ, but also a temperature independent paramagnetism (TIP) and a paramagnetic impurity (P) of a mononuclear complex of Ru(III) with  $S = 1/2$ . Good agreements between the experimental data and calculated curves of the molar susceptibility and magnetic moment have been obtained for compounds **1b**, **2** and **3**. Table 4 collects the calculated magnetic parameters (g, D, zJ, TIP and P) obtained in these fits together with the  $\sigma^2$  value, which indicates the quality of the fits. As an example, Figure 4 shows the experimental and calculated curves using this model for complex **1b**. Similar fits are obtained for complexes **2** and **3** (Figures S2 and S3, Supplementary Materials). The large D calculated values range between 59.66 and 60.31  $\text{cm}^{-1}$ , which are similar to those found for analogous tetracarboxylatodiruthenium(II,III) compounds [1,4,23,33,44,47,48]. The calculated zJ values are between  $-0.09$  and  $-0.32 \text{ cm}^{-1}$ . These low antiferromagnetic coupling constants agree well with the molecular nature of compound **1b** and with the formation of zig-zag chains in **2** and **3**.

**Table 4.** Magnetic parameters obtained in the fits of the magnetic moment versus temperature curves for compounds 1–3.

Compound	g	D/cm <sup>-1</sup>	zJ/cm <sup>-1</sup>	TIP/emu mol <sup>-1</sup>	P/%	σ <sup>2</sup>
<b>1a</b>	2.00 <sup>a,c</sup>	59.25	−11.57	9.83 × 10 <sup>-4</sup>	2.60	8.32 × 10 <sup>-5</sup>
	2.21 <sup>b</sup>	82.23	−14.11	3.40 × 10 <sup>-5</sup>	12.54	1.30 × 10 <sup>-5</sup>
<b>1b</b>	2.22	67.47	−0.16	2.76 × 10 <sup>-7</sup>	2.80	1.07 × 10 <sup>-4</sup>
<b>2</b>	2.12	59.66	−0.09	2.24 × 10 <sup>-4</sup>	2.67 × 10 <sup>-7</sup>	3.24 × 10 <sup>-5</sup>
<b>3</b>	2.02	60.31	−0.32	5.80 × 10 <sup>-3</sup>	0.47	4.46 × 10 <sup>-5</sup>

<sup>a</sup> Considering a Ru(III) monomer as impurity. <sup>b</sup> Considering **1b** as impurity. <sup>c</sup> Fixed parameter.

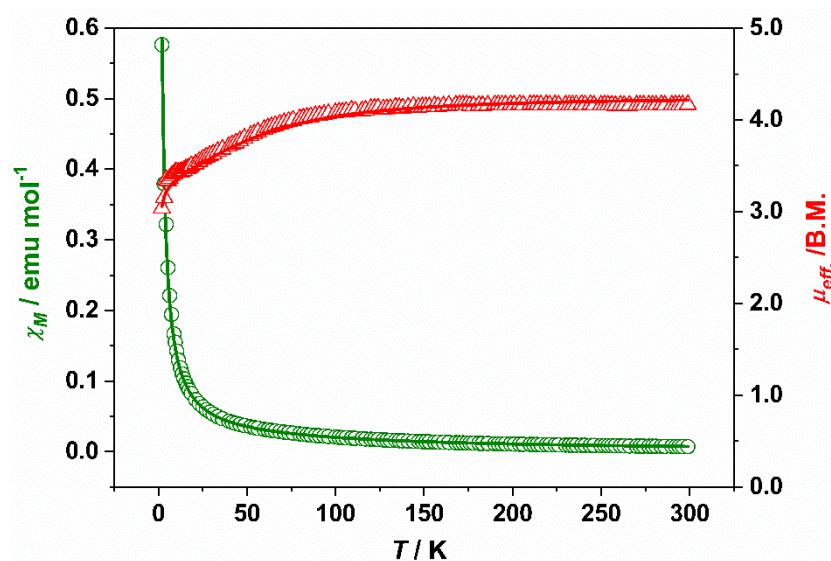


**Figure 4.** Temperature dependence of the molar susceptibility (o) and magnetic moment (Δ) for compound [Ru<sub>2</sub>Cl(μ-O<sub>2</sub>CC<sub>6</sub>H<sub>4</sub>-o-OMe)<sub>4</sub>(EtOH)] (**1b**). Solid lines are the product of a least-squares fit of the experimental data to the model indicated in the text.

Compound **1a** shows a maximum at 49 K in the molar susceptibility vs. temperature curve (Figure 5) and a paramagnetic tail from 13 to 2 K. This behavior indicates a linear chain arrangement in the solid state of the diruthenium units [23,32,49–52]. In this case, there is a strong antiferromagnetic coupling between these units, which are bridged by a chloride ligand giving a 180° Ru-Cl-Ru angle. In this case, the model of Cukiernik [44] is not valid to fit the experimental magnetic data, since this model does not foresee a maximum in the molar susceptibility curve. A suitable model to fit the magnetic data of linear polymeric diruthenium complexes has also been developed previously [49]. This model considers that every  $S = 3/2$  Ru<sub>2</sub><sup>5+</sup> unit has a strong antiferromagnetic coupling with the closest neighbors units, but the couplings are negligible with the rest. For the fit of the magnetic data of **1a**, two different paramagnetic impurities have been taken into account: (a) a Ru(III) monomer with  $S = 1/2$  as it is usual in similar fits (see above) and (b) compound **1b**, i.e., a polymorph of compound **1a** forming discrete molecules with the fixed *g*, *D* and *zJ* values obtained in the fit of **1b**. The results of these fits are also shown in Table 4, where the σ<sup>2</sup> values obtained indicate good agreements between the experimental data and the calculated curves for the two fits. Figures 5 and S4 show, respectively, the experimental and calculated curves considering compound **1b** and a mononuclear Ru(III) as impurity. The calculated *zJ* values are −11.57 cm<sup>-1</sup> (fit a) and −14.11 cm<sup>-1</sup> (fit b). These values are larger than those obtained for compounds **1b**, **2** and **3** and close to those found in similar diruthenium(II,III) complexes with linear Ru-Cl-Ru angles [23,32,49–52]. This is indicative of stronger antiferromagnetic couplings in linear compounds than in molecular or zigzag complexes. The amount of paramagnetic impurity obtained in fit (a) (2.60%) is similar to those obtained for similar linear complexes [23,32,49–52]. Fit b yields a higher impurity percentage (12.54%) but also

a better quality of the fit, considering the higher  $\sigma^2$  value. Since the elemental analysis and the UV-Vis-NIR spectrum indicate that compound **1a** is a chemically pure sample, this paramagnetic impurity is likely a fraction of the same compound with molecular arrangement or zigzag chains. The presence of different polymorphs of the same complex as magnetic impurities has been previously postulated for similar tetracarboxylato [32] and tetraamidatodiruthenium(II,III) [23] complexes.

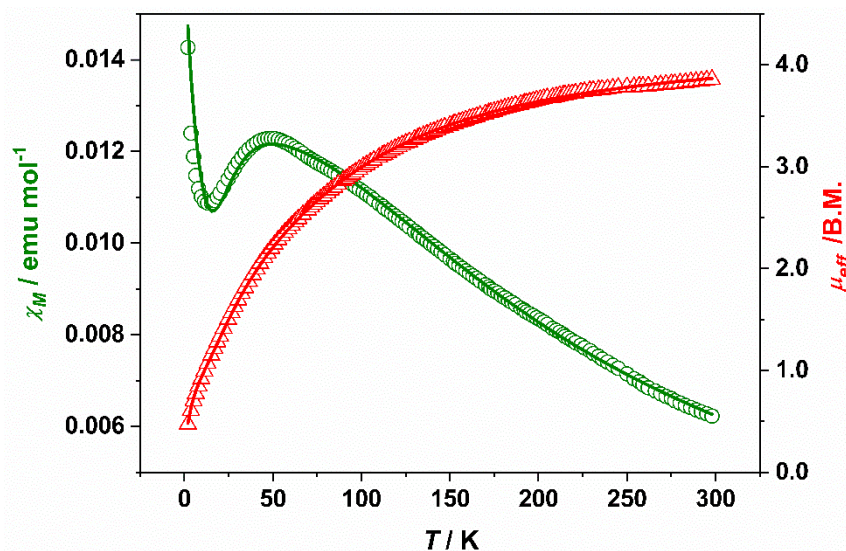


**Figure 5.** Temperature dependence of the molar susceptibility (o) and magnetic moment ( $\Delta$ ) for compound  $[\text{Ru}_2\text{Cl}(\mu\text{-O}_2\text{CC}_6\text{H}_4\text{-}o\text{-OMe})_4]_n$  (**1a**). Solid lines are the product of a least-square fit of the experimental data to the model indicated in the text and considering compound **1b** as the impurity.

In summary, the maximum in the magnetic susceptibility curve for complex **1a** clearly indicates that this complex has a polymeric linear structure. The absence of this maximum in complexes **2** and **3** and its high insolubility in polar and non polar solvents indicate a polymeric zig-zag chains arrangement [1,2,4].

#### 4. Conclusions

The use of the methoxybenzoate ligands has allowed the isolation of diruthenium species as linear polymers (**1a**) zig-zag chains (**2** and **3**), discrete molecules (**1b**) and a salt in which the cation and the anion are diruthenium complexes (**1c**). These arrangements have been found previously, but it is the first time that all of them are obtained with the same ligand. The presence of a  $-\text{OMe}$  substituent in different positions in the phenyl ring must be the cause of the structural diversity found in these complexes. Thus, polymeric compounds of the type  $[\text{Ru}_2\text{Cl}(\mu\text{-O}_2\text{CC}_6\text{H}_4\text{-OMe})_4]_n$  (**1a**, **2** and **3**) with chloride ions bridging the diruthenium units have been prepared independently of the position of the  $-\text{OMe}$  groups in the phenyl ring. However, the steric influence of the  $-\text{OMe}$  group in *ortho* is crucial to obtain compounds **1a**, **1b** and **1c** with different arrangements depending on the synthetic procedure and reaction conditions. Conventional synthesis is the most suitable to obtain compounds **2** and **3**, whereas compounds **1b** and **1c** have been prepared only by solvothermal synthesis. This work demonstrates how important the control of the variables in play is in order to design the required structure for a particular application of the diruthenium species.

**Supplementary Materials:** The following are available online at <https://www.mdpi.com/article/10.3390/app12031000/s1>: Figure S1:  $\theta$  angles between carboxylate plane and aromatic ring plane in **1b**. Figure S2: Temperature dependence of the molar susceptibility (o) and magnetic moment ( $\Delta$ ) for compound  $[\text{Ru}_2\text{Cl}(\mu\text{-O}_2\text{CC}_6\text{H}_4\text{-}m\text{-OMe})_4]_n$  (**2**). Figure S3: Temperature dependence of the molar susceptibility (o) and magnetic moment ( $\Delta$ ) for compound  $[\text{Ru}_2\text{Cl}(\mu\text{-O}_2\text{CC}_6\text{H}_4\text{-}p\text{-OMe})_4]_n$  (**3**).

Figure S4: Temperature dependence of the molar susceptibility ( $\chi$ ) and magnetic moment ( $\Delta$ ) for compound  $[\text{Ru}_2\text{Cl}(\mu\text{-O}_2\text{CC}_6\text{H}_4\text{-}o\text{-OMe})_4]_n$  (**1a**). Table S1:  $\theta$  angles between carboxylate plane and aromatic ring plane in compounds **1b** and **1c**. Table S2: Angles between aromatic ring plane and methoxy substituent plane in compounds **1b** and **1c**.

**Author Contributions:** P.D.-M. and L.M.-M. carried out the synthesis, supervised by R.G.-P. and J.L.P. Conceptualization: R.J.-A., J.L.P. and S.H.; Characterization: P.D.-M., R.G.-P. and J.L.P.; Discussion of the results: all authors; R.G.-P., P.D.-M. and R.J.-A. wrote the original draft, and S.H., J.L.P. and R.J.-A. revised the final manuscript. All authors have read and agreed to the published version of the manuscript.

**Funding:** This research was funded by Comunidad de Madrid (project B2017/BMD-3770-CM) and Ministerio de Ciencia e Innovación (project CTQ2011-23066).

**Conflicts of Interest:** The authors declare no conflict of interest. The funders had no role in the design of the study; in the collection, analyses or interpretation of data; in the writing of the manuscript or in the decision to publish the results.

## References

1. Cotton, F.A.; Murillo, C.A.; Walton, R.A. (Eds.) *Multiple Bonds between Metal Atoms*, 3rd ed.; Springer Science and Business Media: New York, NY, USA, 2005; ISBN 978-0-387-25084-7.
2. Liddle, S.T. (Ed.) *Molecular Metal-Metal Bonds: Compounds, Synthesis, Properties*; Wiley-VCH: Weinheim, Germany, 2015; ISBN 978-3-527-33541-1.
3. Cortijo, M.; González-Prieto, R.; Herrero, S.; Priego, J.L.; Jiménez-Aparicio, R. The Use of Amidinate Ligands in Paddlewheel Diruthenium Chemistry. *Coord. Chem. Rev.* **2019**, *400*, 213040. [[CrossRef](#)]
4. Aquino, M.A.S. Recent Developments in the Synthesis and Properties of Diruthenium Tetracarboxylates. *Coord. Chem. Rev.* **2004**, *248*, 1025–1045. [[CrossRef](#)]
5. Miyazawa, T.; Suzuki, T.; Kumagai, Y.; Takizawa, K.; Kikuchi, T.; Kato, S.; Onoda, A.; Hayashi, T.; Kamei, Y.; Kamiyama, F.; et al. Chiral Paddle-Wheel Diruthenium Complexes for Asymmetric Catalysis. *Nat. Catal.* **2020**, *3*, 851–858. [[CrossRef](#)]
6. Thompson, D.J.; Barker Paredes, J.E.; Villalobos, L.; Ciclosi, M.; Elsy, R.J.; Liu, B.; Fanwick, P.E.; Ren, T. Diruthenium(II,III) Tetracarboxylates Catalyzed  $\text{H}_2\text{O}_2$  Oxygenation of Organic Sulfides. *Inorg. Chim. Acta* **2015**, *424*, 150–155. [[CrossRef](#)]
7. De Oliveira Silva, D. Ruthenium Compounds Targeting Cancer Therapy. In *Frontiers in Anti-Cancer Drug Discovery*; Atta-ur-Rahman, Iqbal Choudhary, M., Eds.; Bentham Science Publishers: Sharjah, United Arab Emirates, 2014; Volume 4, pp. 88–156, ISBN 978-1-60805-922-5.
8. Barresi, E.; Tolbatov, I.; Marzo, T.; Zappelli, E.; Marrone, A.; Re, N.; Pratesi, A.; Martini, C.; Taliani, S.; Settimo, F.D.; et al. Two Mixed Valence Diruthenium(II,III) Isomeric Complexes Show Different Anticancer Properties. *Dalton Trans.* **2021**, *50*, 9643–9647. [[CrossRef](#)] [[PubMed](#)]
9. Coloma, I.; Cortijo, M.; Fernández-Sánchez, I.; Perles, J.; Priego, J.L.; Gutiérrez, C.; Jiménez-Aparicio, R.; Desvoves, B.; Herrero, S. pH- and Time-Dependent Release of Phytohormones from Diruthenium Complexes. *Inorg. Chem.* **2020**, *59*, 7779–7788. [[CrossRef](#)] [[PubMed](#)]
10. Messori, L.; Marzo, T.; Sanches, R.N.F.; Hanif, U.R.; de Oliveira Silva, D.; Merlino, A. Unusual Structural Features in the Lysozyme Derivative of the Tetrakis(Acetato)Chloridodiruthenium(II,III) Complex. *Angew. Chem. Int. Ed.* **2014**, *53*, 6172–6175. [[CrossRef](#)] [[PubMed](#)]
11. Lozano, G.; Jimenez-Aparicio, R.; Herrero, S.; Martinez-Salas, E. Fingerprinting the Junctions of RNA Structure by an Open-Paddlewheel Diruthenium Compound. *RNA* **2016**, *22*, 330–338. [[CrossRef](#)] [[PubMed](#)]
12. Tolbatov, I.; Marrone, A. Reaction of Dirhodium and Diruthenium Paddlewheel Tetraacetate Complexes with Nucleophilic Protein Sites: A Computational Study. *Inorg. Chim. Acta* **2022**, *530*, 120684. [[CrossRef](#)]
13. Malinski, T.; Chang, D.; Feldmann, F.N.; Bear, J.L.; Kadish, K.M. Electrochemical Studies of a Novel Ruthenium(II, III) Dimer, Trifluoroacetamidodiruthenium Chloride ( $\text{Ru}_2(\text{HNOCCF}_3)_4\text{Cl}$ ). *Inorg. Chem.* **1983**, *22*, 3225–3233. [[CrossRef](#)]
14. Barral, M.C.; Jiménez-Aparicio, R.; Priego, J.L.; Royer, E.C.; Urbanos, F.A.; Monge, A.; Ruíz-Valero, C. Tert-Butylbenzamidate Diruthenium(II, III) Compounds. Crystal Structure of  $[\text{Ru}_2(\mu\text{-HNOCC}_6\text{H}_4\text{-}p\text{-CMe}_3)_4(\text{OPPh}_3)_2]\text{BF}_4$ . *Polyhedron* **1993**, *12*, 2947–2953. [[CrossRef](#)]
15. Ryde, K.; Tocher, D.A. The Electro-Oxidation of the Binuclear Ruthenium(II/III) Tetra-Amidate Complex,  $\text{Ru}_2(\text{Me}_3\text{CCONH})_4\text{Cl}$ . *Inorg. Chim. Acta* **1986**, *118*, L49–L51. [[CrossRef](#)]
16. Chakravarty, A.R.; Cotton, F.A.; Tocher, D.A. Synthesis and Structure of a Binuclear Ruthenium 4-Chlorobenzamidato Complex. *Polyhedron* **1985**, *4*, 1097–1102. [[CrossRef](#)]
17. Chavan, M.Y.; Feldmann, F.N.; Lin, X.Q.; Bear, J.L.; Kadish, K.M. Generation of Dinuclear Ruthenium Acetamidate Complexes with Variable Ruthenium-Ruthenium Bond Orders. *Inorg. Chem.* **1984**, *23*, 2373–2375. [[CrossRef](#)]

18. Barral, M.C.; de la Fuente, I.; Jiménez-Aparicio, R.; Priego, J.L.; Torres, M.R.; Urbanos, F.A. Synthesis of Diruthenium(II,III) Amidate Compounds. Crystal Structure of  $[\text{Ru}_2(\mu\text{-HNOCC}_4\text{H}_3\text{S})_4(\text{Thf})_2]\text{SbF}_6 \cdot 0.5\text{cyclohexane}$ . *Polyhedron* **2001**, *20*, 2537–2544. [[CrossRef](#)]
19. Villalobos, L.; Cao, Z.; Fanwick, P.E.; Ren, T. Diruthenium(II,III) Tetramidates as a New Class of Oxygenation Catalysts. *Dalton Trans.* **2011**, *41*, 644–650. [[CrossRef](#)]
20. Herrero, S.; Jiménez-Aparicio, R.; Perles, J.; Priego, J.L.; Urbanos, F.A. First Microwave Synthesis of Multiple Metal-Metal Bond Paddlewheel Compounds. *Green Chem.* **2010**, *12*, 965–967. [[CrossRef](#)]
21. Herrero, S.; Jiménez-Aparicio, R.; Perles, J.; Priego, J.L.; Saguar, S.; Urbanos, F.A. Microwave Methods for the Synthesis of Paddlewheel Diruthenium Compounds with N,N-Donor Ligands. *Green Chem.* **2011**, *13*, 1885–1890. [[CrossRef](#)]
22. González-Prieto, R.; Herrero, S.; Jiménez-Aparicio, R.; Morán, E.; Prado-Gonjal, J.; Priego, J.L.; Schmidt, R. *13. Microwave-Assisted Solvothermal Synthesis of Inorganic Compounds (Molecular and Non Molecular)*; De Gruyter: Berlin, Germany, 2017; pp. 225–247, ISBN 978-3-11-047993-5.
23. Delgado, P.; González-Prieto, R.; Jiménez-Aparicio, R.; Perles, J.; Priego, J.L.; Torres, R.M. Comparative Study of Different Methods for the Preparation of Tetraamidato- and Tetracarboxylatodiruthenium Compounds. Structural and Magnetic Characterization. *Dalton Trans.* **2012**, *41*, 11866–11874. [[CrossRef](#)]
24. Delgado-Martínez, P.; González-Prieto, R.; Gómez-García, C.J.; Jiménez-Aparicio, R.; Priego, J.L.; Torres, M.R. Structural, Magnetic and Electrical Properties of One-Dimensional Tetraamidatodiruthenium Compounds. *Dalton Trans.* **2014**, *43*, 3227–3237. [[CrossRef](#)]
25. Delgado-Martínez, P.; Freire, C.; González-Prieto, R.; Jiménez-Aparicio, R.; Priego, J.; Torres, M. Synthesis, Crystal Structure, and Magnetic Properties of Amidate and Carboxylate Dimers of Ruthenium. *Crystals* **2017**, *7*, 192. [[CrossRef](#)]
26. Delgado-Martínez, P.; Elvira-Bravo, A.; González-Prieto, R.; Priego, J.; Jiménez-Aparicio, R.; Torres, M. Synthesis of  $\text{Ru}_2\text{Br}(\mu\text{-O}_2\text{CC}_6\text{H}_4\text{-R})_4$  (R = o-Me, m-Me, p-Me) Using Microwave Activation: Structural and Magnetic Properties. *Inorganics* **2014**, *2*, 524–536. [[CrossRef](#)]
27. Terán, A.; Cortijo, M.; Gutiérrez, A.; Sánchez-Peláez, A.E.; Herrero, S.; Jiménez-Aparicio, R. Ultrasound-Assisted Synthesis of Water-Soluble Monosubstituted Diruthenium Compounds. *Ultrason. Sonochemistry* **2021**, *80*, 105828. [[CrossRef](#)]
28. Das, B.K.; Chakravarty, A.R. The First Structurally Characterized Diruthenium(II,III) Complex with Four Bridging Arylcarboxylato Ligands. *Polyhedron* **1991**, *10*, 491–494. [[CrossRef](#)]
29. Stephenson, T.A.; Wilkinson, G. New Ruthenium Carboxylate Complexes. *J. Inorg. Nucl. Chem.* **1966**, *28*, 2285–2291. [[CrossRef](#)]
30. Urbanos, F.A. *Program MASAS V 3.1*; UCM: Madrid, Spain, 2002.
31. Barral, M.C.; Jiménez-Aparicio, R.; Priego, J.L.; Royer, E.C.; Urbanos, F.A.; Amador, U. Diruthenium(II,III) Carboxylate Compounds: Existence of Both Polymeric and Ionic Forms in Solution and Solid State. *Inorg. Chem.* **1998**, *37*, 1413–1416. [[CrossRef](#)] [[PubMed](#)]
32. Barral, M.C.; González-Prieto, R.; Jiménez-Aparicio, R.; Priego, J.L.; Torres, M.R.; Urbanos, F.A. Polymeric, Molecular, and Cation/Anion Arrangements in Chloro-, Bromo-, and Iododiruthenium(II,III) Carboxylate Compounds. *Eur. J. Inorg. Chem.* **2003**, *2003*, 2339–2347. [[CrossRef](#)]
33. Aquino, M. Diruthenium and Diosmium Tetracarboxylates: Synthesis, Physical Properties and Applications. *Coord. Chem. Rev.* **1998**, *170*, 141–202. [[CrossRef](#)]
34. Barral, M.C.; Jiménez-Aparicio, R.; Priego, J.L.; Royer, E.C.; Urbanos, F.A. Liquid Secondary Ion Mass Spectrometric Study of Diruthenium(II,III) Complexes. *Inorg. Chim. Acta* **1998**, *277*, 76–82. [[CrossRef](#)]
35. Miskowski, V.M.; Loehr, T.M.; Gray, H.B. Electronic and Vibrational Spectra of  $\text{Ru}_2(\text{Carboxylate})_4^+$  Complexes. Characterization of a High-Spin Metal-Metal Ground State. *Inorg. Chem.* **1987**, *26*, 1098–1108. [[CrossRef](#)]
36. Miskowski, V.M.; Gray, H.B. Electronic Spectra of  $\text{Ru}_2(\text{Carboxylate})_4^+$  Complexes. Higher Energy Electronic Excited States. *Inorg. Chem.* **1988**, *27*, 2501–2506. [[CrossRef](#)]
37. Miskowski, V.M.; Hopkins, M.D.; Winkler, J.R.; Gray, H.B. Multiple Metal-Metal Bonds. In *Inorganic Electronic Structure and Spectroscopy, Volume II: Applications and Case Studies*; Solomon, E.I., Lever, A.B.P., Eds.; Wiley: New York, NY, USA, 1999; pp. 343–402, ISBN 978-0-471-32683-0.
38. Barral, M.C.; González-Prieto, R.; Jiménez-Aparicio, R.; Priego, J.L.; Torres, M.R.; Urbanos, F.A. Synthesis, Properties, and Structural Characterization of Bromo- and Iodotetracarboxylatodiruthenium(II,III) Compounds. *Eur. J. Inorg. Chem.* **2004**, *2004*, 4491–4501. [[CrossRef](#)]
39. Clark, R.J.H.; Franks, M.L. Resonance Raman Spectra of Chlorotetra-Acetato- and Chlorotetrabutyrato-Diruthenium. *J. Chem. Soc. Dalton Trans.* **1976**, 1825–1828. [[CrossRef](#)]
40. Clark, R.J.H.; Ferris, L.T.H. Resonance Raman, Excitation Profile and Electronic Structural Studies of Diruthenium Tetracarboxylate Complexes. *Inorg. Chem.* **1981**, *20*, 2759–2766. [[CrossRef](#)]
41. Castro, M.A.; Roitberg, A.E.; Cukiernik, F.D. Theoretical and Experimental Studies of Diruthenium Tetracarboxylates Structure, Spectroscopy, and Electrochemistry. *Inorg. Chem.* **2008**, *47*, 4682–4690. [[CrossRef](#)] [[PubMed](#)]
42. Cotton, F.A.; Walton, R.A. *Multiple Bonds between Metal Atoms*, 2nd ed.; Clarendon Press: New York, NY, USA; Oxford University Press: Oxford, UK, 1993; ISBN 978-0-19-855649-7.
43. Norman, J.G.; Renzoni, G.E.; Case, D.A. Electronic Structure of  $\text{Ru}_2(\text{O}_2\text{CR})_4^+$  and  $\text{Rh}_2(\text{O}_2\text{CR})_4^+$  Complexes. *J. Am. Chem. Soc.* **1979**, *101*, 5256–5267. [[CrossRef](#)]

44. Cukiernik, F.D.; Luneau, D.; Marchon, J.-C.; Maldivi, P. Mixed-Valent Diruthenium Long-Chain Carboxylates. 2. Magnetic Properties. *Inorg. Chem.* **1998**, *37*, 3698–3704. [[CrossRef](#)] [[PubMed](#)]
45. O'Connor, C.J. Magnetochemistry—Advances in Theory and Experimentation. In *Progress in Inorganic Chemistry*; John Wiley & Sons, Ltd.: Hoboken, NJ, USA, 1982; pp. 203–283, ISBN 978-0-470-16630-7.
46. Telsler, J.; Drago, R.S. Reinvestigation of the Electronic and Magnetic Properties of Ruthenium Butyrate Chloride. *Inorg. Chem.* **1984**, *23*, 3114–3120; Correction in **1985**, *24*, 4765. [[CrossRef](#)]
47. Mikuriya, M.; Yoshioka, D.; Handa, M. Magnetic Interactions in One-, Two-, and Three-Dimensional Assemblies of Dinuclear Ruthenium Carboxylates. *Coord. Chem. Rev.* **2006**, *250*, 2194–2211. [[CrossRef](#)]
48. Estiú, G.; Cukiernik, F.D.; Maldivi, P.; Poizat, O. Electronic, Magnetic, and Spectroscopic Properties of Binuclear Diruthenium Tetracarboxylates: A Theoretical and Experimental Study. *Inorg. Chem.* **1999**, *38*, 3030–3039. [[CrossRef](#)]
49. Jiménez-Aparicio, R.; Urbanos, F.A.; Arrieta, J.M. Magnetic Properties of Diruthenium(II,III) Carboxylate Compounds with Large Zero-Field Splitting and Strong Antiferromagnetic Coupling. *Inorg. Chem.* **2001**, *40*, 613–619. [[CrossRef](#)] [[PubMed](#)]
50. Cotton, F.A.; Kim, Y.; Ren, T. Molecular Structure and Magnetic Properties of a Linear Chain Compound,  $\text{Ru}_2(\text{O}_2\text{CCMePh}_2)_4\text{Cl}$ . *Polyhedron* **1993**, *12*, 607–611. [[CrossRef](#)]
51. Olea, D.; González-Prieto, R.; Priego, J.L.; Barral, M.C.; de Pablo, P.J.; Torres, M.R.; Gómez-Herrero, J.; Jiménez-Aparicio, R.; Zamora, F. MMX Polymer Chains on Surfaces. *Chem. Commun.* **2007**, 1591–1593. [[CrossRef](#)] [[PubMed](#)]
52. Welte, L.; González-Prieto, R.; Olea, D.; Torres, M.R.; Priego, J.L.; Jiménez-Aparicio, R.; Gómez-Herrero, J.; Zamora, F. Time-Dependence Structures of Coordination Network Wires in Solution. *ACS Nano* **2008**, *2*, 2051–2056. [[CrossRef](#)] [[PubMed](#)]